Adaptive reduced basis strategy for rare events simulations

L. Gallimard

Received 26 April 2016; | Revised 6 June 2016; | Accepted 6 June 2016

DOI: xxx/xxxx

ARTICLE TYPE

Adaptive reduced basis strategy for rare events simulations†

L. Galllimard*

[1] UPL, Univ. Paris Nanterre, LEME, Laboratoire Energétique Mécanique Electromagnétisme, 50 rue de Sèvres 92410 Ville d'Avray, France

Correspondence
*L. Galllimard, Email: laurent.gallimard@parisnanterre.fr

Present Address

Summary

Monte-Carlo methods are well suited to characterize events of which associated probabilities are not too low with respect to the simulation budget. For very seldom observed events, these approaches do not lead to accurate results. Indeed, the number of samples are often insufficient to estimate such low probabilities (at least 10^{n+2} samples are needed to estimate a probability of 10^{-n} with 10% relative deviation of the Monte-Carlo estimator). Even within the framework of reduced order methods, such as a reduced basis approach, it seems difficult to accurately predict low probability events. In this paper we propose to combine a cross-entropy method with a reduced basis algorithm to compute rare events (failure) probabilities.

KEYWORDS:
Structural reliability; Finite element analysis; model reduction ; reduced basis ; error bounds ; failure probability; Rare events simulations, cross-entropy

1 | INTRODUCTION

Many applications in structural analysis require taking into account stochastic properties of material, geometry or loads. Given a probabilistic description of the stochastic properties of the structure (i.e. a random vector Θ associated with a probability density function f), reliability analysis aims at computing the probability of failure of structures with respect to a prescribed limit state function G. The failure is defined as an event $F = \{G(\Theta) \leq 0\}$ and the failure probability P_f is defined by $P_f = Prob(\{G(\Theta) \leq 0\}) = \int_{G(\theta)\leq 0} f(\boldsymbol{\theta}) d\boldsymbol{\theta}$. The computation of this failure probability by a standard Monte-Carlo algorithm is too computationally expensive in practice (10^{n+2} finite element computations are need to estimate a probability of failure $P_f = 10^{-n}$). In order to reduce the number of simulations runs different alternatives have been proposed.

A first approach is the First Order Reliability Method (FORM) and the Second Order Reliability Method (SORM)[1,2] which consists in building a simple analytical approximation of the limit-state function around the so-called design point followed by a direct estimation of the failure probability[3,4,5,6,7,8]. A second approach consists in building a surface response as a surrogate model of the limit state function (Quadratic response surfaces, polynomial chaos expansions, kriging surrogates, ...)[9,10,11,12,13]. The Monte-Carlo algorithm can then be applied on this surrogate model. A third approach consists in building a reduced order model (ROM) of the full order finite element model (FOM)[14,15,16,17,18,19], and using the Monte-Carlo method along with the reduced order model. This approach has been applied successfully in[20,21] to compute the failure probability of structures in the case where P_f is greater than 10^{-4}, however in the case of rare events estimation the number of Monte-Carlo simulations needed to estimate accurately P_f increases (10^8 simulations to estimate a failure probability of $P_f = 10^{-6}$) and the computational cost becomes too important even in the context of the use of reduced order models. In order to reduce the number of samples different techniques have been developed[22], in particular the objective of the importance sampling (IS) method is to reduce the variance of the Monte-Carlo estimator. The main idea is to generate the samples Θ_1, ..., Θ_N with an auxiliary probability density function h that is able to generate more samples such that $G(\Theta) \leq 0$ than the probability density function (PDF) f and

† Adaptive reduced basis strategy for rare events simulations.

then to introduce a weight in the probability estimate to take into account the change in the PDF generating samples. The cross entropy (CE) optimization method[23] provides an efficient way to approximate this auxiliary probability density function. In[24] the authors propose to combine a CE method with a surrogate model of the limit state function and to use an exact computation of the limit state function only when the sample is near the failure limit. In[25] the authors develop a CE method with an adaptive surrogate model based on a Kriging interpolation method for estimating the probability of rare events. In[26] the authors propose to use an a priori fixed hierarchy of surrogate models to accelerate the estimation of the auxiliary probability density function h by the CE algorithm, then compute the IS probability estimate with the FOM.

In this work we develop an adaptive strategy, based on the computation of an error estimator of the limit state function, to simultaneously build the reduced basis and the auxiliary probability density function h. The reduced basis vectors are chosen in order to control the quality of the estimation of the limit state function G and the auxiliary PDF is built by minimizing the cross-entropy with respect to an ideal zero-variance distribution. An importance sampling Monte-Carlo simulation is then run with the surrogate model defined by the reduced basis and the auxiliary PDF. The control of the quality of the reduced basis is ensured by the computation of a lower bound and an upper bound of the failure probability. Compared to[24,26], this paper introduces, during the CE optimization, an adaptive construction of the surrogate model based on an error estimator. Compared to[25] it introduces surrogates models based on a reduced basis approximation which allows building bounds of the limit state function as well as of the computed Monte-Carlo failure probability.

The paper is organized as follows: Section 2 describes the problem to be solved. In Section 3 the cross-entropy optimization applied to importance sampling is presented. In Section 4, the reduced basis formulation used to solve the problem is presented as well as the technique used to compute bounds on quantities of interest. The reduced basis algorithm for rare events simulations is detailed in Section 5. Finally, Section 6 presents an application to multilayered structures in 2D plane elasticity.

2 | PROBLEM FORMULATION

2.1 | Linear elastic model

Let us consider a 2D elastic structure defined in a domain Ω bounded by Γ. The external actions on the structure are represented by a surface force density $\mathbf{T}$ defined over a subset Γ_N of the boundary such that $\mathbf{T} \in \left[L^2(\Gamma_N)\right]^2$ and a body force density $\mathbf{b}$ defined in Ω such that $\mathbf{b} \in \left[L^2(\Omega)\right]^2$. We assume that a prescribed displacement $\mathbf{u} = \mathbf{u}_d$ such that $\mathbf{u}_d \in \left[H^{1/2}(\Gamma_D)\right]^2$ is imposed on $\Gamma_D = \Gamma - \Gamma_N$. The material is assumed to be linear elastic, being $\mathbf{C}$ the Hooke tensor. We consider that the problem is dependent of a vector $\boldsymbol{\theta} = (\theta_1, ..., \theta_p) \in \mathcal{D} \subset \mathbb{R}^p$ of uncertain independent parameters. These parameters are characterized in a probabilistic manner by means of a joint probability density function $f(\boldsymbol{\theta}) = \prod_{i=1}^{p} f_i(\theta_i)$, where f_i is the probability function of θ_i. The problem can be formulated as:

1. For any $\boldsymbol{\theta} \in \mathcal{D}$, find a displacement field $\mathbf{u} \in \mathcal{U}$ and a stress field $\boldsymbol{\sigma}$ defined in Ω which verify:

   - the kinematic constraints:
   $$\mathbf{u}(x, \boldsymbol{\theta}) = \mathbf{u}_d(x) \text{ on } \Gamma_D \tag{1}$$
   - the equilibrium equations:
   $$\mathbf{div}\, \boldsymbol{\sigma}(x, \boldsymbol{\theta}) + \mathbf{b}(x, \boldsymbol{\theta}) = \mathbf{0} \text{ in } \Omega \text{ and } \boldsymbol{\sigma}(x, \boldsymbol{\theta})\mathbf{n} = \mathbf{T}(x, \boldsymbol{\theta}) \text{ on } \Gamma_N \tag{2}$$
   - the constitutive equation:
   $$\boldsymbol{\sigma}(x, \boldsymbol{\theta}) = \mathbf{C}(x, \boldsymbol{\theta})\boldsymbol{\epsilon}(\mathbf{u}(x, \boldsymbol{\theta})) \text{ in } \Omega \tag{3}$$

   $\mathbf{n}$ denotes the outer normal to Ω. $\mathcal{U}$ is the space in which the displacement field is being sought, $\mathcal{U}^0$ the space of the fields in $\mathcal{U}$ which are zero on Γ_D, and $\boldsymbol{\epsilon}(\mathbf{u})$ denotes the linearized deformation associated with the displacement: $[\boldsymbol{\epsilon}(\mathbf{u})]_{ij} = 1/2\,(u_{i,j} + u_{j,i})$.

2. Compute a quantity of interest:
   $$S(\theta) = Q(\mathbf{u}(x, \boldsymbol{\theta})) \tag{4}$$
   where Q is a linear output of $\mathbf{u}$

Remark: For the sake of simplicity assume that $\mathbf{u}_d$ is a deterministic value (i.e. $\mathbf{u}_d(x,\boldsymbol{\theta}) = \mathbf{u}_d(x)$). For an interested reader, the development of a reduced basis algorithm where $\mathbf{u}_d$ is also described by a stochastic approach can be found in [27].

The weak form formulation of the problem (Equations 1-3) is: find $\mathbf{u} \in \mathcal{U}$ such that

$$a(\mathbf{u}(\boldsymbol{\theta}), \mathbf{u}^*; \boldsymbol{\theta}) = l(\mathbf{u}^*; \boldsymbol{\theta}) \quad \forall \mathbf{u}^* \in \mathcal{U}^0 \tag{5}$$

where

$$a(\mathbf{u}(\boldsymbol{\theta}), \mathbf{u}^*; \boldsymbol{\theta}) = \int_\Omega \mathbf{C}(x,\boldsymbol{\theta})\boldsymbol{\varepsilon}(\mathbf{u}(x,\boldsymbol{\theta})) : \boldsymbol{\varepsilon}(\mathbf{u}^*(x))\, d\Omega \text{ and } l(\mathbf{u}^*; \boldsymbol{\theta}) = \int_\Omega \mathbf{b}(x,\boldsymbol{\theta}).\mathbf{u}^*(x)\, d\Omega + \int_{\Gamma_N} \mathbf{T}(x,\boldsymbol{\theta}).\mathbf{u}^*(x)\, d\Gamma$$

To compute the solution $\mathbf{u}(\boldsymbol{\theta})$ of Equation (5), a finite element approximation $\mathbf{u}_h$ of $\mathbf{u}$ is introduced such that $\mathbf{u}_h \in \mathcal{U}_h \subset \mathcal{U}$. Let $\mathcal{P}_h$ be a partition of Ω into elements E_k ($k \in \{1, ..., N_{FE}\}$). This partition formed by the union of all elements, is assumed to coincide exactly with the domain Ω and any two elements are either disjoint or share a common edge. We assume that $\mathbf{u}_d$ can be represented by a displacement field in $\mathcal{U}_h$. The discretized problem is: Find a displacement field $\mathbf{u}_h(\boldsymbol{\theta}) \in \mathcal{U}_h$ and a stress field $\boldsymbol{\sigma}_h(\boldsymbol{\theta})$ defined in Ω which verify:

- the kinematic constraints:

$$\mathbf{u}_h(\mathbf{x}, \boldsymbol{\theta}) = \mathbf{u}_d(\mathbf{x}) \text{ on } \Gamma_D \tag{6}$$

- the finite element equilibrium equations:

$$\int_\Omega \boldsymbol{\sigma}_h(\boldsymbol{\theta}) : \boldsymbol{\varepsilon}(\mathbf{u}_h^*)\, d\Omega = \int_\Omega \mathbf{b}(\boldsymbol{\theta}).\mathbf{u}_h^*\, d\Omega + \int_{\Gamma_N} \mathbf{T}(\boldsymbol{\theta}).\mathbf{u}_h^* d\Gamma \quad \forall \mathbf{u}_h^* \in \mathcal{U}_h^0 \tag{7}$$

- the constitutive equation:

$$\boldsymbol{\sigma}_h(\mathbf{x}, \boldsymbol{\theta}) = \mathbf{C}(\mathbf{x}, \boldsymbol{\theta})\boldsymbol{\varepsilon}(\mathbf{u}_h(\mathbf{x}, \boldsymbol{\theta})) \text{ in } \Omega \tag{8}$$

The classical weak form formulation is: find $\mathbf{u}_h \in \{\mathbf{v} \in \mathcal{U}_h;\ \mathbf{v}_{|\Gamma_D} = \mathbf{u}_d\}$ such that:

$$a(\mathbf{u}_h(\boldsymbol{\theta}), \mathbf{u}_h^*; \boldsymbol{\theta}) = l(\mathbf{u}_h^*; \boldsymbol{\theta}) \quad \forall \mathbf{u}_h^* \in \mathcal{U}_h^0 \tag{9}$$

where $\mathcal{U}_h^0 = \{\mathbf{v} \in \mathcal{U}_h; \mathbf{v}\,|_{\Gamma_D} = \mathbf{0}\}$.

Following [28], we assume that the Hooke tensor $\mathbf{C}$, the body forces $\mathbf{b}$ and the traction forces $\mathbf{T}$ can be decomposed as the sum of functions of $\boldsymbol{\theta}$ multiplied by deterministic functions.

$$\mathbf{C}(\mathbf{x}, \boldsymbol{\theta}) = \sum_{q=1}^{Q^c} \Theta_q^c(\boldsymbol{\theta})\bar{\mathbf{C}}_q(\mathbf{x}), \quad \mathbf{b}(\mathbf{x}, \boldsymbol{\theta}) = \sum_{q=1}^{Q^b} \Theta_q^b(\boldsymbol{\theta})\bar{\mathbf{b}}_q(\mathbf{x}) \quad \mathbf{T}(\mathbf{x}, \boldsymbol{\theta}) = \sum_{q=1}^{Q^T} \Theta_q^T(\boldsymbol{\theta})\bar{\mathbf{T}}_q(\mathbf{x}) \tag{10}$$

where $\Theta_q^c, \Theta_q^b, \Theta_q^T$ are known functions of $\boldsymbol{\theta}$, each $\bar{\mathbf{C}}_q(\mathbf{x})$ is a fourth order tensor defined in Ω, $\bar{\mathbf{b}}_q(\mathbf{x})$ are vector fields defined in Ω, and $\bar{\mathbf{T}}_q(\mathbf{x})$ are vector fields defined on Γ_N.

Remark: An approximation of this decomposition can be obtained by the use of the Karhunen-Loeve expansion [29] as proposed in [30].

Furthermore, we assume that the inverse of the Hooke tensor can be decomposed as the sum of functions of $\boldsymbol{\theta}$ multiplied by deterministic functions defined in Ω.

$$\mathbf{C}^{-1}(\mathbf{x}, \boldsymbol{\theta}) = \sum_{q=1}^{Q^s} \Theta_q^s(\boldsymbol{\theta})\bar{\mathbf{S}}_q(\mathbf{x}) \tag{11}$$

where each $\bar{\mathbf{S}}_q(\mathbf{x})$ is a fourth order tensor defined on Ω. These hypotheses are required by the adaptive reduced basis method [21] as shown in section 4.2.

2.2 | Structural reliability model

In this section, we describe the problem of reliability assessment [1,31,10]. Let us denote by $S(\boldsymbol{\theta}) = Q(\mathbf{u}_h(x, \boldsymbol{\theta}))$ the computational output of interest and $R(\boldsymbol{\theta})$ the threshold associated to this computational output. Classically the structure failure state is defined by a limit state function:

$$G(\boldsymbol{\theta}) = R(\boldsymbol{\theta}) - S(\boldsymbol{\theta}) \tag{12}$$

such that

- $G(\boldsymbol{\theta}) < 0$ is a failure state for the structure,
- $G(\boldsymbol{\theta}) = 0$ is the limit state,
- $G(\boldsymbol{\theta}) > 0$ is a safe state for the structure.

According to this definition, the system fails when G is lower or equal to zero. The failure probability P_f is then given by:

$$P_f = \int\limits_{D_f = \{\boldsymbol{\theta} \in \mathbb{R}^n ; G(\boldsymbol{\theta}) \leq 0\}} f(\boldsymbol{\theta})\, d\boldsymbol{\theta} \tag{13}$$

where n is the dimension of the vector $\boldsymbol{\theta}$ and $f(\boldsymbol{\theta})$ is a PDF. The evaluation of the integral defined by Equation (13) is not easy because it represents a very small quantity and because the integration domain is defined implicitly. Monte-Carlo algorithm is the main approach to solve the reliability problem. Recasting Equation (13) as:

$$P_f = \int\limits_{\mathbb{R}^n} \mathbf{1}_{(G(\boldsymbol{\theta}) \leq 0)}(\boldsymbol{\theta}) f(\boldsymbol{\theta})\, d\boldsymbol{\theta} = E_f\left[\mathbf{1}_{(G(\boldsymbol{\theta}) \leq 0)}\right] \tag{14}$$

where $\mathbf{1}_{(G(\boldsymbol{\theta}) \leq 0)}$ is the failure indicator function being equal to one if $G(\boldsymbol{\theta}) \leq 0$ and zero otherwise. The probability of failure is equal to the expectation of $\mathbf{1}_{(G(\boldsymbol{\theta}) \leq 0)}$. The Monte-Carlo algorithm consists in generating a number N_{MC} of realizations $\boldsymbol{\theta}^n$ of the random vector Θ using the actual probability density function, then in computing the Monte-Carlo estimator $\hat{P}_f$:

$$\hat{P}_f = \frac{1}{N_{MC}} \sum_{n=1}^{N_{MC}} \mathbf{1}_{(G(\boldsymbol{\theta}) \leq 0)}(\boldsymbol{\theta}^n) \tag{15}$$

According to the central limit theorem, this estimator is asymptotically unbiased and normally distributed with variance

$$Var\left[\hat{P}_f\right] = \frac{\hat{P}_f(1 - \hat{P}_f)}{N_{MC} - 1}$$

When the failure probability is small the relative deviation of the estimator is

$$\delta = \frac{\sqrt{Var\left[\hat{P}_f\right]}}{\hat{P}_f} \approx \frac{1}{\sqrt{N_{MC}\, \hat{P}_f}} \tag{16}$$

The relative deviation is consequently unbounded. From Equation (16), it can be seen that obtaining a relative deviation $\delta \leq 10\%$ for a probability of failure of 10^{-n} requires about 10^{n+2} finite element simulations.

3 | IMPORTANCE SAMPLING

3.1 | Principles

The objective of importance sampling [32,33,34] is to reduce the variance of the Monte-Carlo estimator $\hat{P}_f$. The idea is to generate the samples $\boldsymbol{\theta}^1, ..., \boldsymbol{\theta}^N$ with an auxiliary PDF h such that the generated samples have a higher rate of falling in the failure region than with the PDF f, because only these samples contribute to the evaluation of P_f.

$$P_f = E_f\left[\mathbf{1}_{(G(\boldsymbol{\theta}) \leq 0)}\right] = \int \mathbf{1}_{(G(\boldsymbol{\theta}) \leq 0)} f(\boldsymbol{\theta}) d\boldsymbol{\theta} = \int \mathbf{1}_{(G(\boldsymbol{\theta}) \leq 0)} \frac{f(\boldsymbol{\theta})}{h(\boldsymbol{\theta})} h(\boldsymbol{\theta})\, d\boldsymbol{\theta} = E_h\left[\mathbf{1}_{(G(\boldsymbol{\theta}) \leq 0)} \frac{f(\boldsymbol{\theta})}{h(\boldsymbol{\theta})}\right] \tag{17}$$

Let us denote $w(\boldsymbol{\theta}) = \frac{f(\boldsymbol{\theta})}{h(\boldsymbol{\theta})}$, then the failure probability is estimated by

$$\hat{P}_f^{IS} = \frac{1}{N}\sum_{n=1}^{N} \mathbf{1}_{(G(\boldsymbol{\theta}^n)\leq 0)} w(\boldsymbol{\theta}^n) \tag{18}$$

where $\hat{P}_f^{IS}$ is called the importance sampling (IS) estimator. The variance of this estimator is given by the following equation

$$Var(\hat{P}_f^{IS}) = \frac{Var\left(\mathbf{1}_{(G(\boldsymbol{\theta})\leq 0)} w(\boldsymbol{\theta})\right)}{N} \tag{19}$$

The optimal choice for h is given by

$$h^*(\boldsymbol{\theta}) = \frac{\mathbf{1}_{(G(\boldsymbol{\theta})\leq 0)} f(\boldsymbol{\theta})}{P_f} \tag{20}$$

which leads to

$$\mathbf{1}_{(G(\boldsymbol{\theta})\leq 0)} w(\boldsymbol{\theta}) = \mathbf{1}_{(G(\boldsymbol{\theta})\leq 0)} \left(f(\boldsymbol{\theta}) \frac{P_f}{\mathbf{1}_{(G(\boldsymbol{\theta})\leq 0)} f(\boldsymbol{\theta})} \right) = P_f \tag{21}$$

and hence to $Var(\hat{P}_f^{IS}) = 0$. The obvious difficulty of this approach is that h^* depends not only on the failure domain which is unknown, but also on the unknown probability P_f. Nevertheless, a good sampling density h will be close to the PDF h^*.

3.2 | Cross-Entropy approach to determine a good Importance Sampling distribution

The idea of the Cross-Entropy (CE)[35,36,23] is to choose the IS density h in a specified class of densities such that the cross-entropy or Kullback-Leiber (K-L) divergence between the optimal importance sampling density h^* and h is minimal. The K-L divergence between two PDF f and g is given by:

$$\mathcal{D}(f,g) = E_f\left[\ln \frac{f(\boldsymbol{\theta})}{g(\boldsymbol{\theta})}\right] = \int f(\boldsymbol{\theta}) \ln \frac{f(\boldsymbol{\theta})}{g(\boldsymbol{\theta})} d\boldsymbol{\theta} = \int f(\boldsymbol{\theta}) \ln f(\boldsymbol{\theta}) d\boldsymbol{\theta} - \int f(\boldsymbol{\theta}) \ln g(\boldsymbol{\theta}) d\boldsymbol{\theta} \tag{22}$$

Let us define h_λ a family of PDF indexed by the parameter λ (λ could be the mean and the covariance matrix in case of Gaussian densities). The objective is then to find λ^* which minimizes the Kullback-Leiber divergence $\mathcal{D}(h^*, h_\lambda)$

$$\lambda^* = \underset{\lambda}{\operatorname{argmin}}\, \mathcal{D}(h^*, h_\lambda) = \underset{\lambda}{\operatorname{argmin}} \left(-\int h^*(\boldsymbol{\theta}) \ln h_\lambda(\boldsymbol{\theta}) d\boldsymbol{\theta} \right) \tag{23}$$

substituting $h^*(\boldsymbol{\theta})$ from Equation (20) in Equation (23) we obtain

$$\lambda^* = \underset{\lambda}{\operatorname{argmax}} \int \left(\mathbf{1}_{(G(\boldsymbol{\theta})\leq 0)} f(\boldsymbol{\theta})\right) \ln h_\lambda(\boldsymbol{\theta}) d\boldsymbol{\theta} = \underset{\lambda}{\operatorname{argmax}}\, E_f\left[\mathbf{1}_{(G(\boldsymbol{\theta})\leq 0)} \ln h_\lambda(\boldsymbol{\theta})\right] \tag{24}$$

Remark: In[23], it is shown that solving the cross-entropy problem defined by Equation (23) yields an estimate with minimum variance.

λ^* can be estimated by solving the following stochastic program

$$\lambda^* = \underset{\lambda}{\operatorname{argmax}} \frac{1}{N_{CE}} \sum_{n=1}^{N_{CE}} \mathbf{1}_{(G(\boldsymbol{\theta}^n)\leq 0)} \frac{f(\boldsymbol{\theta}^n)}{h_\lambda(\boldsymbol{\theta}^n)} \ln h_\lambda(\boldsymbol{\theta}^n) \tag{25}$$

where $\boldsymbol{\theta}^1, ..., \boldsymbol{\theta}^{N_{CE}}$ are N_{CE} random samples generated according to the probability density h_λ. In practice, ones does not solve directly Equation (25) since it requires the knowledge of several samples such that $G(\boldsymbol{\theta}^n) \leq 0$, which is not the case for rare event evaluation. To circumvent this difficulty, the optimization problem (25) is solved by a multilevel iterative method[35,23] with a decreasing sequence of thresholds $G_0 > G_1 > ... \geq 0$ chosen adaptively using a quantile definition. At each iteration, the value of λ_{k-1} is available and ones determine in practice

$$\lambda_k = \underset{\lambda}{\operatorname{argmax}} \frac{1}{N_{CE}} \sum_{n=1}^{N_{CE}} \mathbf{1}_{(G(\boldsymbol{\theta}^n)\leq G_k)} \frac{f(\boldsymbol{\theta}^n)}{h_{k-1}(\boldsymbol{\theta}^n)} \ln h_\lambda(\boldsymbol{\theta}^n) \tag{26}$$

The algorithm is initialized by choosing a parameter ρ (typically $10^{-2} \leq \rho \leq 10^{-1}$, see[35,23] for more details), and by defining $h_0 = f$. At each iteration k of the algorithm N_{CE} samples $\boldsymbol{\theta}^1, ..., \boldsymbol{\theta}^{N_{CE}}$ are generated according the probability density h_{k-1}, the values of the limit state function $G(\boldsymbol{\theta}^n)$ are computed and G_k is set to the $\max(0, G_\rho)$ where G_ρ is the value of the ρ-quantile of

$\left(G(\boldsymbol{\theta}^1), ...G(\boldsymbol{\theta}^{N_{CE}})\right)$. Then, Equation (26) is solved and we set $h_k = h_{\lambda_k}$. Let K be the final iteration when $G_K = 0$, N_{IS} samples $\boldsymbol{\theta}^1, ..., \boldsymbol{\theta}^{N_{IS}}$ are generated according to the probability density h_{λ_K} and the importance sampling estimator is computed by

$$\hat{P}_f^{IS} = \frac{1}{N_{IS}} \sum_{n=1}^{N_{IS}} \mathbf{1}_{(G(\boldsymbol{\theta}^n)\leq 0)} \frac{f(\boldsymbol{\theta}^n)}{h_K(\boldsymbol{\theta}^n)} \tag{27}$$

The Cross-Entropy algorithm is described in Algorithm 1.

Remark: The maximization of Equation (26) can often be solved analytically, in particular when the probability density family is composed by independent Gaussian or log-normal random variables, as used in this paper (see section 6).

Algorithm 1 Pseudocode for the IS based on a CE optimization

input: the PDF f, N_{CE} (number of samples used for the CE optimization), N_{IS} (number of samples used for the IS estimation), ρ a parameter in $[10^{-2}, 10^{-1}]$
output: $\hat{P}_f^{IS}$

Define $h_0 = f$. Set G_0 such that $G_0 > 0$.
Set $k = 0$ (iteration counter)
while $G_k > 0$ **do**
  Set $k = k + 1$
  Generate random samples $\left(\boldsymbol{\theta}^1, .., \boldsymbol{\theta}^{N_{CE}}\right)$ according to the probability density h_{k-1}. Compute $G(\boldsymbol{\theta}^n)$ (for $n = 1, N_{CE}$).
  Compute $G_k = \max(0, G_\rho)$, where G_ρ is the ρ-quantile of $\left(G(\boldsymbol{\theta}^1), ..., G(\boldsymbol{\theta}^{N_{CE}})\right)$
  Use $\left(\boldsymbol{\theta}^1, .., \boldsymbol{\theta}^{N_{CE}}\right)$ and $\left(G(\boldsymbol{\theta}^1), ..., G(\boldsymbol{\theta}^{N_{CE}})\right)$ to solve

$$\lambda^* = \underset{\lambda}{\operatorname{argmax}} \frac{1}{N_{CE}} \sum_{n=1}^{N_{CE}} \mathbf{1}_{(G(\boldsymbol{\theta}^n)\leq G_k)} \frac{f(\boldsymbol{\theta}^n)}{h_{k-1}(\boldsymbol{\theta}^n)} \ln h_\lambda(\boldsymbol{\theta}^n)$$

  Set $\lambda_k = \lambda^*$ and $h_k = h_{\lambda_k}$.
end while
Set $h_{opt} = h_k$
Generate N_{IS} samples according to the probability density h_{opt} and compute $\hat{P}_f^{IS}$

$$\hat{P}_f^{IS} = \frac{1}{N_{IS}} \sum_{n=1}^{N_{IS}} \mathbf{1}_{(G(\boldsymbol{\theta}^n)\leq 0)} \frac{f(\boldsymbol{\theta}^n)}{h_{opt}(\boldsymbol{\theta}^n)}$$

3.3 | Simple 1D example

A simple 1D test problem proposed in [18] is considered here to illustrate the CE algorithm. The unknown displacement $u(x, \boldsymbol{\theta})$ describes the deformation of a bar of section S and length L which is loaded by a traction F on $x = L$ and clamped at $x = 0$ (see Fig 1). The random parameters are the Young modulus E of the bar and the traction F. They are functions of two independent Gaussian random variables (θ_1, θ_2) defined in Table 1

$$E(\theta_1) = E_0(1 + \delta g(\theta_1)) \text{ with } g(\theta_1) = \frac{2 \arcsin(\text{Erf}(\frac{\theta_1}{\sqrt{2}}))}{\sqrt{\pi^2 - 8}}$$

and

$$F(\theta_2) = \theta_2$$

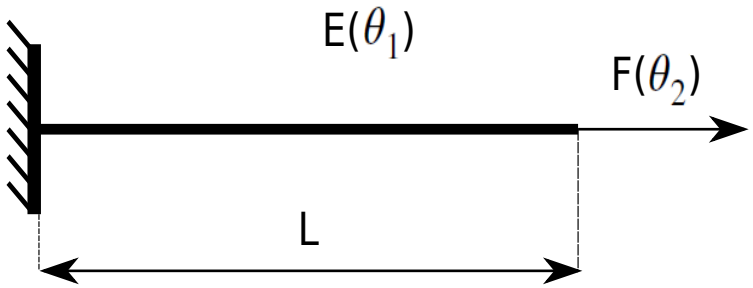

FIGURE 1 Unidimensional bar

Remark: The nonlinear mapping g is chosen such that the probability density function of $E(\theta_1)$ has a bounded support. Actually, the upper and lower limits for E are

$$E_0\left(1-\delta\sqrt{\frac{\pi^2}{\pi^2-8}}\right) \leq E(\theta_1) \leq E_0\left(1+\delta\sqrt{\frac{\pi^2}{\pi^2-8}}\right)$$

This definition allows precluding negative non-physical values of the Young modulus if $0 \leq \delta < \sqrt{\frac{\pi^2-8}{\pi^2}}$.

Random variable	distribution	mean value	standard deviation
θ_1	Gaussian	m_1	σ_1
θ_2	Gaussian	m_2	σ_2

TABLE 1 Statistical properties of the random variables

The limit state function is given by

$$G(\theta_1,\theta_2) = u_c - u(L,\theta_1,\theta_2)$$

The analytical expression of the quantity of interest is easily available

$$u(L,\theta_1,\theta_2) = \frac{F(\theta_2)L}{E(\theta_1)S}$$

The PDF f in this example is given as a function of the mean values and the standard deviations of θ_1, θ_2.

$$f(\theta_1,\theta_2;m_1,\sigma_1,m_2,\sigma_2) = \prod_{i=1}^{2}\frac{1}{\sqrt{2}\sigma_i}\exp\left(-\frac{1}{2}\left(\frac{\theta_i-m_i}{\sigma_i}\right)^2\right) \tag{28}$$

The family of PDF to be optimized for the parameter $\lambda = (\tilde{m}_1,\tilde{\sigma}_1,\tilde{m}_2,\tilde{\sigma}_2)$ will be defined by

$$h(\theta_1,\theta_2;\tilde{m}_1,\tilde{\sigma}_1,\tilde{m}_2,\tilde{\sigma}_2) = \prod_{i=1}^{2}\frac{1}{\sqrt{2}\tilde{\sigma}_i}\exp\left(-\frac{1}{2}\left(\frac{\theta_i-\tilde{m}_i}{\tilde{\sigma}_i}\right)^2\right) \tag{29}$$

As an example we consider the following values:

- Geometrical values: $L = 1$, $S = 0.1$.
- Young's modulus: $E_0 = 200$, $\delta = 0.3$, $m_1 = 0$, $\sigma_1 = 1$.
- Applied traction: $m_2 = 1$, $\sigma_2 = 0.1$.
- Critical displacement: $u_c = 0.1$

A standard Monte-Carlo method with 10^6 samples gives an estimate $\hat{P}_f = 1.48 \times 10^{-4}$, with a relative deviation $\delta = 8.2\%$. With 10^7 samples we obtain an estimate $\hat{P}_f = 1.54 \times 10^{-4}$, with a relative deviation $\delta = 2.5\%$. For the IS method based on CE

k	G_k	$\tilde{m}_1$	$\tilde{\sigma}_1$	$\tilde{m}_2$	$\tilde{\sigma}_2$
1	0.058	0	1	0.5	0.1
2	0.022	−1.64	0.66	0.56	0.086
3	0.00014	−2.59	0.37	0.64	0.060
4	0	−3.10	0.46	0.73	0.055

TABLE 2 Convergence of the CE optimization

optimization we use the following parameters: $\rho = 0.1$, $N_{CE} = 10^3$ and $N_{IS} = 10^4$. Table 2 displays the results of the CE optimization.

Using the estimated optimal parameter vector $\lambda_4 = (-3.10, 0.46, 0.73, 0.055)$, the final iteration with $N_{IS} = 10^4$ samples gives an estimate of $\hat{P}_f^{IS} = 1.51 \times 10^{-4}$, with a relative deviation $\delta = 1.5\%$. In this case for an equivalent relative deviation we have reduced our simulation effort by a factor 10^3. However, in practical mechanical computation it is mandatory to reduce the cost of generation of each sample. The aim of the section 4, is to introduce the so-called reduced basis method.

4 | REDUCED BASIS METHOD

The purpose of a Reduced Basis Method is to provide a fast evaluation $\mathbf{u}_{rb}(\boldsymbol{\theta})$ of the value of the displacement field $\mathbf{u}_h(\boldsymbol{\theta})$ and hence a fast evaluation $Q(\mathbf{u}_{rb}(\boldsymbol{\theta}); \boldsymbol{\theta})$ of any quantity of interest $Q(\mathbf{u}_h(\boldsymbol{\theta}); \boldsymbol{\theta})$. In this section we recall a classical displacement approach which consists in performing a Galerkin projection onto a reduced basis space that is assumed to represent accurately the solutions of the problem to be solved. The construction of this reduced basis space, that will be detailed in section 5, is aimed to control the accuracy of the computed failure probability. To control this accuracy we define and compute an error estimator which is an upper bound of the error on the quantity of interest $|Q(\mathbf{u}_h(\boldsymbol{\theta}); \boldsymbol{\theta}) - Q(\mathbf{u}_{rb}(\boldsymbol{\theta}); \boldsymbol{\theta})|$. The computation of this upper bound necessitates the construction of a stress field that satisfies the finite element equilibrium equations (Equations 7). Following the approach developed in[21], in order to obtain a fast evaluation of this stress field, we propose in section 4.1 to build, from the displacement reduced basis, a stress reduced basis which satisfies the finite element equilibrium equations. In this paper, we use a reduced basis strategy which permits to control the quality of the reliability analysis which was proposed in[21]. We present the main ingredients of this strategy in the following subsections.

4.1 | Offline Phase

Let $\mathbf{u}_{dir} \in \mathcal{U}_h$ be a displacement field such that $\mathbf{u}_{dir|\Gamma_D} = \mathbf{u}_d$. Let us introduce a set of samples in the parameter space $\mathcal{S}^{N_s} = \{\boldsymbol{\theta}^1, \dots, \boldsymbol{\theta}^{N_s}\}$, where $\boldsymbol{\theta}^n \in \mathcal{D}$, and for each $\boldsymbol{\theta}^n$ compute a finite element solution $\mathbf{u}_h^0(\boldsymbol{\theta}^n)$ in $\mathcal{U}_h^0$ described by the corresponding vector of nodal values $\mathbf{q}^n$.

$$a(\mathbf{u}_h^0(\boldsymbol{\theta}^n), \mathbf{u}_h^*; \boldsymbol{\theta}^n) = f(\mathbf{u}_h^*; \boldsymbol{\theta}^n) - a(\mathbf{u}_{dir}, \mathbf{u}_h^*; \boldsymbol{\theta}^n) \quad \forall \mathbf{u}_h^* \in \mathcal{U}_h^0 \tag{30}$$

On this space, following[37,38,39], we perform a Gram-Schmidt orthonormalization process for the inner product $a(\mathbf{u}, \mathbf{v}; \bar{\boldsymbol{\theta}})$ ($\bar{\boldsymbol{\theta}}$ being a fixed value of the random vector which is selected a priori as shown in Section 5.1). The reduced basis space is then defined by

$$\mathcal{U}_{rb}^{0,N_s} = \text{span}\,\{\boldsymbol{\phi}^1, \dots, \boldsymbol{\phi}^{N_s}\} \subset \mathcal{U}_h^0 \tag{31}$$

The choice of the samples in the parameter space $\mathcal{S}^{N_s}$ and of the associated reduced basis $\mathcal{U}_{rb}^{0,N_s}$ depends on the sampling strategy (see[38] for more details).

To construct the stress reduced basis, we follow the method presented in[21]. The first step consists in building a stress $\boldsymbol{\sigma}_{neu}(\boldsymbol{\theta})$ which verifies the F.E. equilibrium (Equation 7) for all $\boldsymbol{\theta}$ in $\mathcal{D}$ (We refer the reader to[21] for more details about the construction of $\boldsymbol{\sigma}_{neu}(\boldsymbol{\theta})$). Let us consider the set of stress fields computed from the snapshot solutions (Equation 30)

$$\boldsymbol{\sigma}_{rb}^n = \mathbf{C}(\boldsymbol{\theta}^n)\boldsymbol{\epsilon}(\mathbf{u}_h^0(\boldsymbol{\theta}^n) + \mathbf{u}_{dir}) \text{ for } n \in \{1, \dots, N_s\} \tag{32}$$

and the set of stress fields defined by

$$\Delta\boldsymbol{\sigma}_{rb}^n = \boldsymbol{\sigma}_{rb}^n - \boldsymbol{\sigma}_{neu}(\boldsymbol{\theta}^n) \tag{33}$$

It follows that $\{\Delta\boldsymbol{\sigma}^n_{rb}, \text{ for } n \in \{1, \dots, N_s\}\}$ is a set of stress fields equilibrated to zero in the FE sense. An orthonormal basis $\mathcal{S}^{0,N_s}_{rb} = \{\boldsymbol{\zeta}^1, \dots, \boldsymbol{\zeta}^{N_s}\}$ is built from $\Delta\boldsymbol{\sigma}^n_{rb}$ by a Gram-Schmidt process with respect to an internal product $\int_\Omega \boldsymbol{\sigma}_1 : \mathbf{C}^{-1}(\bar{\boldsymbol{\theta}})\boldsymbol{\sigma}_2 \, d\Omega$.

4.2 | Online Phase

The reduced basis approximation consists in solving Equation (5) in $\mathcal{U}^0_{rb} + \{\mathbf{u}_{dir}\}$. A key point to justify the use of the reduced basis approximation is that N_s is assumed to be much smaller than the number of degree of freedom of the F.E. model N_{FE} (i.e. $N_s << N_{FE}$). The reduced basis solution for the displacement field writes

$$\mathbf{u}_{rb}(\boldsymbol{\theta}) = \mathbf{u}_{dir} + \sum_{n=1}^{N_s} \alpha_n \boldsymbol{\phi}^n \tag{34}$$

The coefficients α_n are computed by solving

$$a(\mathbf{u}^0_{rb}(\boldsymbol{\theta}), \mathbf{u}^*_{rb}; \boldsymbol{\theta}) = f(\mathbf{u}^*_{rb}; \boldsymbol{\theta}) - a(\mathbf{u}_{dir}, \mathbf{u}^*_{rb}; \boldsymbol{\theta}) \quad \forall \mathbf{u}^*_{rb} \in \mathcal{U}^0_{rb} \tag{35}$$

which leads to an algebraic system

$$[\mathbf{K}(\boldsymbol{\theta})]\,[\boldsymbol{\alpha}] = [\mathbf{F}(\boldsymbol{\theta})] \tag{36}$$

The elements of $[\mathbf{K}(\boldsymbol{\theta})]$ and of $[\mathbf{F}(\boldsymbol{\theta})]$ are defined by

$$K_{ij}(\boldsymbol{\theta}) = a(\boldsymbol{\phi}^i, \boldsymbol{\phi}^j; \boldsymbol{\theta}) \text{ and } F_i(\boldsymbol{\theta}) = f(\boldsymbol{\phi}^i; \boldsymbol{\theta}) \tag{37}$$

Thanks to the decomposition (Equation 10) of $\mathbf{C}$, $\mathbf{b}$ and $\mathbf{T}$, K_{ij} and F_i can be written as a linear combination of the functions $\Theta^c_q(\boldsymbol{\theta})$, $\Theta^b_q(\boldsymbol{\theta})$ and $\Theta^T_q(\boldsymbol{\theta})$

$$K_{ij}(\boldsymbol{\theta}) = \sum_{q=1}^{Q^c} \bar{K}_{ijq}\Theta^q_c(\boldsymbol{\theta}) \text{ and } F_i(\boldsymbol{\theta}) = \sum_{q=1}^{Q^b} \bar{b}_{iq}\Theta^b_q(\boldsymbol{\theta}) + \sum_{q=1}^{Q^T} \bar{T}_{iq}\Theta^T_q(\boldsymbol{\theta}) \tag{38}$$

where

$$\bar{K}_{ijq} = \int_\Omega \bar{\mathbf{C}}_q \boldsymbol{\varepsilon}(\boldsymbol{\phi}^i) : \boldsymbol{\varepsilon}(\boldsymbol{\phi}^j) d\Omega, \quad \bar{b}_{iq} = \int_\Omega \bar{\mathbf{b}}_q . \boldsymbol{\phi}^i d\Omega, \text{ and } \bar{T}_{iq} = \int_{\Gamma_N} \bar{\mathbf{T}}_q . \boldsymbol{\phi}^i d\Gamma$$

The reduced basis solution for the stress field writes

$$\boldsymbol{\sigma}^e_{rb}(\boldsymbol{\theta}) = \boldsymbol{\sigma}_{neu}(\boldsymbol{\theta}) + \sum_{n=1}^{N_s} \beta_n \boldsymbol{\zeta}^n \tag{39}$$

The coefficients β_n are computed in order to minimize a distance between the stress field $\boldsymbol{\sigma}_{rb}(\boldsymbol{\theta})$ computed from the reduced basis solution $\mathbf{u}_{rb}(\boldsymbol{\theta})$ through the constitutive equation ($\boldsymbol{\sigma}_{rb}(\boldsymbol{\theta}) = \mathbf{C}(\boldsymbol{\theta})\boldsymbol{\varepsilon}(\mathbf{u}_{rb}(\boldsymbol{\theta}))$) and $\boldsymbol{\sigma}^e_{rb}(\boldsymbol{\theta})$

$$\boldsymbol{\sigma}^e_{rb}(\boldsymbol{\theta}) = \underset{(\beta_1,\dots,\beta_{N_s})}{\operatorname{argmin}} \, \eta(\theta) \tag{40}$$

where

$$\eta(\theta) = \int_\Omega (\boldsymbol{\sigma}_{rb}(\boldsymbol{\theta}) - \boldsymbol{\sigma}^e_{rb}(\boldsymbol{\theta})) : \mathbf{C}^{-1}(\boldsymbol{\theta})(\boldsymbol{\sigma}_{rb}(\boldsymbol{\theta}) - \boldsymbol{\sigma}^e_{rb}(\boldsymbol{\theta})) \, d\Omega \tag{41}$$

The minimization of Equation (40) leads to the algebraic system

$$[\mathbf{S}(\boldsymbol{\theta})]\,[\boldsymbol{\beta}] = [\mathbf{G}(\boldsymbol{\theta})] \tag{42}$$

The elements of $[\mathbf{S}(\boldsymbol{\theta})]$ and of $[\mathbf{G}(\boldsymbol{\theta})]$ are defined by

$$S_{ij} = \int_\Omega \mathbf{C}^{-1}(\boldsymbol{\theta})\boldsymbol{\zeta}^j : \boldsymbol{\zeta}^i \, d\Omega \tag{43}$$

and

$$G_i = \int_\Omega \boldsymbol{\zeta}^i : (\boldsymbol{\varepsilon}(\mathbf{u}_{rb}) - \mathbf{C}^{-1}(\boldsymbol{\theta})\boldsymbol{\sigma}_{neu}(\boldsymbol{\theta})) \, d\Omega \tag{44}$$

Thanks to the decompositions (Equation 10) and (Equation 11) S_{ij} and G_i can be written as a linear combination of the functions $\Theta^s_q(\boldsymbol{\theta})$, $\Theta^b_q(\boldsymbol{\theta})$ and $\Theta^T_q(\boldsymbol{\theta})$

$$S_{ij} = \sum_{q=1}^{Q^s} \bar{S}_{ijq}\Theta^s_q(\boldsymbol{\theta})$$

$$G_i = \bar{c}_{i0} + \sum_{j=1}^{N_s} \bar{c}_{ij}\alpha_j - \sum_{j=1}^{Q^s}\left(\sum_{q=1}^{Q^b} \bar{b}_{ijq}\Theta_j^s(\theta)\Theta_q^b(\theta) + \sum_{q=1}^{Q^T} \bar{T}_{ijq}\Theta_j^s(\theta)\Theta_q^T(\theta)\right)$$

where

$$\bar{S}_{ijq} = \int_\Omega \mathbf{S}^q\boldsymbol{\zeta}^i : \boldsymbol{\zeta}^j \, d\Omega, \quad \bar{c}_{i0} = \int_\Omega \boldsymbol{\zeta}^i : \boldsymbol{\varepsilon}(\mathbf{u}_{dir}) \, d\Omega, \quad \bar{c}_{ij} = \int_\Omega \boldsymbol{\zeta}^i : \boldsymbol{\varepsilon}(\boldsymbol{\phi}^j) \, d\Omega$$

and

$$\bar{b}_{ijq} = \int_\Omega \boldsymbol{\zeta}^i : \bar{\mathbf{S}}_j\mathbf{C}(\bar{\theta})\boldsymbol{\varepsilon}(\mathbf{u}_q^b) d\Omega, \quad \bar{T}_{ijq} = \int_{\Gamma_N} \boldsymbol{\zeta}^i : \bar{\mathbf{S}}_j\mathbf{C}(\bar{\theta})\boldsymbol{\varepsilon}(\mathbf{u}_q^T) d\Gamma$$

4.3 | Error estimator and bounds on the quantity of interest

The computation of error bounds on linear Quantities of Interest (QoI) has been developed by many authors[40,41,42,43,44] for measuring the gap between an exact QoI and a QoI computed from a finite element analysis. The error bounds between a QoI computed from a finite element analysis and a QoI computed by a reduced modeling approach have been studied since early 2000[45,16,19,46,47]. In this paper, we use the bounds proposed in[48,21] within the framework of the application of the error in the constitutive relation to reduced basis computations. These bounds are obtained by using the parallelogram inequality as proposed in[41,45].

For any realization of the random vector $\boldsymbol{\theta}$ the error introduced by the reduced approximation is given by

$$\mathbf{e}_{rb}(\boldsymbol{\theta}) = \mathbf{u}_h(\boldsymbol{\theta}) - \mathbf{u}_{rb}(\boldsymbol{\theta}) \tag{45}$$

due to the linearity assumption, one has

$$Q(\mathbf{e}_{rb}(\boldsymbol{\theta});\boldsymbol{\theta}) = Q(\mathbf{u}_h(\boldsymbol{\theta});\boldsymbol{\theta}) - Q(\mathbf{u}_{rb}(\boldsymbol{\theta});\boldsymbol{\theta}) \tag{46}$$

Following[44], we consider the following auxiliary problem: find $\mathbf{u}_h^{aux} \in \mathcal{U}_h^0$ such that:

$$a(\mathbf{u}_h^*, \mathbf{u}_h^{aux}(\boldsymbol{\theta});\boldsymbol{\theta}) = Q(\mathbf{u}_h^*(\boldsymbol{\theta});\boldsymbol{\theta}) \quad \forall\, \mathbf{u}_h^* \in \mathcal{U}_h^0 \tag{47}$$

and its solution $\mathbf{u}_{rb}^{aux}$ in the reduced basis

$$a(\mathbf{u}_{rb}^{aux}(\boldsymbol{\theta}), \mathbf{u}_{rb}^*;\boldsymbol{\theta}) = Q(\mathbf{u}_{rb}^*;\boldsymbol{\theta}) \quad \forall \mathbf{u}_{rb}^* \in \mathcal{U}_{rb}^0 \tag{48}$$

It can be shown that (we refer the reader to[43,49,48,21] for more details)

$$-e_{rb}^-(\boldsymbol{\theta}) \le Q(\mathbf{e}_{rb}(\boldsymbol{\theta});\boldsymbol{\theta}) \le e_{rb}^+(\boldsymbol{\theta}) \tag{49}$$

where

$$e_{rb}^+(\boldsymbol{\theta}) = \tfrac{1}{2}\left(\|\boldsymbol{\sigma}_{rb}^e(\boldsymbol{\theta}) - \boldsymbol{\sigma}_{rb}(\boldsymbol{\theta})\|_{\sigma,\theta}\, \|\boldsymbol{\sigma}_{rb}^{aux,e}(\boldsymbol{\theta}) - \boldsymbol{\sigma}_{rb}^{aux}(\boldsymbol{\theta})\|_{\sigma,\theta} + < \boldsymbol{\sigma}_{rb}^e(\boldsymbol{\theta}) - \boldsymbol{\sigma}_{rb}(\boldsymbol{\theta}), \boldsymbol{\sigma}_{rb}^{aux,e}(\boldsymbol{\theta}) - \boldsymbol{\sigma}_{rb}^{aux}(\boldsymbol{\theta}) >_{\sigma,\theta}\right)$$

$$e_{rb}^-(\boldsymbol{\theta}) = \tfrac{1}{2}\left(\|\boldsymbol{\sigma}_{rb}^e(\boldsymbol{\theta}) - \boldsymbol{\sigma}_{rb}(\boldsymbol{\theta})\|_{\sigma,\theta}\, \|\boldsymbol{\sigma}_{rb}^{aux,e}(\boldsymbol{\theta}) - \boldsymbol{\sigma}_{rb}^{aux}(\boldsymbol{\theta})\|_{\sigma,\theta} - < \boldsymbol{\sigma}_{rb}^e(\boldsymbol{\theta}) - \boldsymbol{\sigma}_{rb}(\boldsymbol{\theta}), \boldsymbol{\sigma}_{rb}^{aux,e}(\boldsymbol{\theta}) - \boldsymbol{\sigma}_{rb}^{aux}(\boldsymbol{\theta}) >_{\sigma,\theta}\right)$$

$\boldsymbol{\sigma}_{rb}(\boldsymbol{\theta})$ and $\boldsymbol{\sigma}_{rb}^{aux}(\boldsymbol{\theta})$ are the stresses computed from the reduced basis solutions $\mathbf{u}_{rb}(\boldsymbol{\theta})$ and $\mathbf{u}_{rb}^{aux}(\boldsymbol{\theta})$ through the constitutive equation, $\boldsymbol{\sigma}_{rb}^e(\boldsymbol{\theta})$ and $\boldsymbol{\sigma}_{rb}^{aux,e}(\boldsymbol{\theta})$ are stress fields equilibrated in the FE sense which are computed, for a given value of $\boldsymbol{\theta}$, as proposed in section (4.2). $\|\sigma\|_{\sigma,\theta}$ is defined by

$$\|\sigma\|_{\sigma,\theta}^2 = < \boldsymbol{\sigma}, \boldsymbol{\sigma} >_{\sigma,\theta} \text{ with } < \boldsymbol{\sigma}_1, \boldsymbol{\sigma}_2 >_{\sigma,\theta} = \int_\Omega \boldsymbol{\sigma}_1 : \mathbf{C}^{-1}(\boldsymbol{\theta})\boldsymbol{\sigma}_2 \, d\Omega$$

From Equations (46) and (49) it follows that the quantity of interest $Q(\mathbf{u}_h(\boldsymbol{\theta});\boldsymbol{\theta})$ is bounded by

$$Q(\mathbf{u}_{rb}(\boldsymbol{\theta});\boldsymbol{\theta}) - e_{rb}^-(\boldsymbol{\theta}) \le Q(\mathbf{u}_h(\boldsymbol{\theta});\boldsymbol{\theta}) \le Q(\mathbf{u}_{rb}(\boldsymbol{\theta});\boldsymbol{\theta}) + e_{rb}^+(\boldsymbol{\theta}) \tag{50}$$

Remark: If Q does not depend linearly on u_h, bounding of the quantity interest is much more difficult and there are few works addressing the subject (see[37,19] for quadratic outputs or[50] for mean von Mises stress over a subdomain).

4.4 | Bounds of the limit state and on the failure probability

The approximate limit state function computed from the reduced basis analysis is

$$G_{rb}(\boldsymbol{\theta}) = R(\boldsymbol{\theta}) - Q(\mathbf{u}_{rb}(\boldsymbol{\theta}); \boldsymbol{\theta}) \tag{51}$$

The approximate failure probability computed by a Monte-Carlo method is given by

$$\hat{P}_f^{rb} = \frac{1}{N_{MC}} \sum_{n=1}^{N_{MC}} \mathbf{1}_{(G_{rb}(\boldsymbol{\theta})\leq 0)}(\boldsymbol{\theta}^n) \tag{52}$$

and from Equation (50) the following computable bounds of the limit state function $G(\boldsymbol{\theta})$ are obtained

$$G_{rb}^-(\boldsymbol{\theta}) \leq G(\boldsymbol{\theta}) \leq G_{rb}^+(\boldsymbol{\theta}) \tag{53}$$

where

$$G_{rb}^-(\boldsymbol{\theta}) = G_{rb}(\boldsymbol{\theta}) - e_{rb}^+(\boldsymbol{\theta}) \text{ and } G_{rb}^+(\boldsymbol{\theta}) = G_{rb}(\boldsymbol{\theta}) + e_{rb}^-(\boldsymbol{\theta}) \tag{54}$$

Let us introduce the failure domain associated with the lower bound and the upper bound of the limit-state function and the associated failure probabilities

$$\mathcal{D}_f^+ = \{\boldsymbol{\theta};\, G_{rb}(\boldsymbol{\theta}) - e_{rb}^+(\boldsymbol{\theta}) \leq 0\} \text{ and } \mathcal{D}_f^- = \{\boldsymbol{\theta};\, G_{rb}(\boldsymbol{\theta}) + e_{rb}^-(\boldsymbol{\theta}) \leq 0\}$$

$$\hat{P}_f^+ = \frac{1}{N_{MC}} \sum_{n=1}^{N_{MC}} \mathbf{1}_{\mathcal{D}_f^+}(\boldsymbol{\theta}^n) \text{ and } \hat{P}_f^- = \frac{1}{N_{MC}} \sum_{n=1}^{N_{MC}} \mathbf{1}_{\mathcal{D}_f^-}(\boldsymbol{\theta}^n) \tag{55}$$

As $\mathcal{D}_f^- \subset \mathcal{D}_f = \{\boldsymbol{\theta}; G(\boldsymbol{\theta}) \leq 0\} \subset \mathcal{D}_f^+$ we obtain the following bounds for the failure probability

$$\hat{P}_f^- \leq \hat{P}_f \leq \hat{P}_f^+ \tag{56}$$

Remark: It must be noticed that the obtained bounds concern the failure probability $\hat{P}_f$ computed from a Monte-Carlo algorithm. The quality of the Monte-Carlo estimator will be classically assessed in the examples presented in section 6 via the central limit theorem and the computation of the relative deviation δ (Equation 16).

Furthermore, to control the reduced basis algorithm an error estimator $\varepsilon_G(\boldsymbol{\theta})$, which is an upper bound on the error on the limit state function $e_G(\boldsymbol{\theta}) = |G(\boldsymbol{\theta}) - G_{rb}(\boldsymbol{\theta})|$, is introduced

$$e_G(\boldsymbol{\theta}) \leq \varepsilon_G(\boldsymbol{\theta}) = \max(e_{rb}^-(\boldsymbol{\theta}), e_{rb}^+(\boldsymbol{\theta})) \tag{57}$$

Properties:

1. If for all $\boldsymbol{\theta}^n, \varepsilon_G(\boldsymbol{\theta}^n) = 0$ then $\hat{P}_f^- = \hat{P}_f^+ = \hat{P}_f$.
2. If $\hat{P}_f^- = \hat{P}_f^+$ then $\varepsilon_G(\boldsymbol{\theta}^n) = 0$ for all $\boldsymbol{\theta}^n$ and $\hat{P}_f = \hat{P}_f^- = \hat{P}_f^+$.

5 | REDUCED BASIS ALGORITHM FOR RARE EVENTS SIMULATIONS

The Monte-Carlo method (see Section 2.2 and Equation 15) is the reference method to compute the failure probability. To evaluate a failure probability $P_f = 10^{-n}$ with a relative deviation $\delta = 10\%$ the Monte-Carlo method necessitates 10^{n+2} FOM computations. To reduce the computational effort it is interesting to introduce reduced order models based on the RB method[20,21]. As shown in Section 4, this method involves the construction of a basis (the so-called reduced basis). The construction of this reduced basis can be performed offline in a training space as proposed in[20] or adaptively during the Monte-Carlo simulation as proposed in[21]. In any case 10^{n+2} ROM computations are performed in order to evaluate the failure probability P_f. For rare events simulations, it is mandatory to reduce not only the cost of the computations but also their number. The method developed here proposes to reduce the number of samples needed by using an IS estimator along with the reduced basis approximation. In Section 3, we presented the CE method for computing an IS optimized distribution. The idea of the method proposed in this paper is to build the reduced basis while the iterations of the CE method are performed. As, at each iteration k the optimization process involves only the samples $\boldsymbol{\theta}$ such that the limit-state function $G(\boldsymbol{\theta})$ is below a given threshold G_k (Equation 26), the reduced basis approximation is improved only when these samples are not computed with a sufficient accuracy in the actual reduced basis.

Compared to a classical MC-IS algorithm, the advantage of the proposed algorithm is that the computations of the IS failure probability is done with a ROM rather than a FOM. Compared to a classical MC-RB algorithm, the advantage of the proposed algorithm is that the number of computations of Monte-Carlo samples performed in the ROM is greatly reduced.

1. Offline stage : Construct the reduced bases while performing the iterations of the CE algorithm.
2. Online stage : Compute the importance sampling estimator, together with its inferior bound and superior bound, with the reduced bases defined in step 1.

5.1 | Offline stage

The initial step of the algorithm consists in computing a displacement field $\mathbf{u}_{dir}$ satisfying the boundary conditions (Equation 6) and a stress field $\boldsymbol{\sigma}_{neu}(\boldsymbol{\theta})$ satisfying the equilibrium in the FE sense (Equation 7). The computation of $\mathbf{u}_{dir}$ and $\boldsymbol{\sigma}_{neu}(\boldsymbol{\theta})$ involves the choice of a particular value of $\boldsymbol{\theta}$ denoted $\bar{\boldsymbol{\theta}}$, a simple choice is to use the mean value of the random vector $\bar{\boldsymbol{\theta}} = E_f[\boldsymbol{\theta}]$. This value will also be used in the Gram-Schmidt orthonormalization algorithm. The idea is to construct the reduced bases along with the CE optimization process. For each sample $\boldsymbol{\theta}^n$ generated during the CE optimization, an approximate solution $\mathbf{u}_{rb}(\boldsymbol{\theta}^n)$ of $\mathbf{u}_h(\boldsymbol{\theta}^n)$ is computed in the reduced basis space $\mathcal{U}_{rb}^{0,n_{rb}}$. The approximate limit state function $G_{rb}(\boldsymbol{\theta}^n)$ is computed as well as its upper bound $G_{rb}^+(\boldsymbol{\theta}^n)$ and lower bound $G_{rb}^-(\boldsymbol{\theta}^n)$. Two cases must be distinguished:

- If $G_{rb}^-(\boldsymbol{\theta}^n) > G_{k-1}$ then $G(\boldsymbol{\theta}^n) > G_{k-1}$ and this sample will not contribute to the optimization problem (Eq 58).
- If $G_{rb}^-(\boldsymbol{\theta}^n) \leq G_{k-1}$ this sample may or may not contribute to the optimization problem (Eq 58).

In the first case the quality of value of $G_{rb}(\boldsymbol{\theta}^n)$ provided by the reduced basis $\mathcal{U}_{rb}^{0,n_{rb}}$ is sufficient and the simulations are continued on the same reduced basis. In the second case, the reduced bases $\mathcal{U}_{rb}^{0,n_{rb}}$ and $\mathcal{S}_{rb}^{0,n_{rb}}$ are improved only if the error estimator on the limit state function is greater than a fixed tolerance $\varepsilon_G(\boldsymbol{\theta}^n) \geq \tau_{CE}$; in this case the problem is solved in the finite element space and new reduced basis spaces $\mathcal{U}_{rb}^{0,n_{rb}+1}$ and $\mathcal{S}_{rb}^{0,n_{rb}+1}$ are constructed. When the values of $G(\boldsymbol{\theta}^1), ..., G(\boldsymbol{\theta}^{N_{CE}})$ have been computed, we compute their ρ-quantile G_k and we optimize the parameters λ in order to minimize the Kullback-Leibler divergence between the auxiliary PDF h_λ and the optimal auxiliary PDF for the limit-state function defined by the threshold G_k: $G(\boldsymbol{\theta}) = G_k$. The algorithm is given in Algorithm (2).

It must be noticed that the reduced bases are constructed iteratively for decreasing thresholds $G_1 > G_2 > ... > G_k > 0$, whereas our actual limit-state function is defined by $G(\boldsymbol{\theta}) = 0$. To obtain bases which accurately describe the limit-state function, a new iteration of the optimization process is added. In this iteration, we add vectors in the reduced bases when the RB accuracy is insufficient to certify the state of the structure, and we optimize the parameters λ in order to minimize the Kullback-Leibler divergence between the auxiliary PDF h_λ and the optimal auxiliary PDF for the limit-state function $G(\boldsymbol{\theta}) = 0$. The algorithm is given in Algorithm 4. In this stage, the reduced bases are increased when the error estimator on the limit state function is greater than a fixed tolerance τ_{CE}^L with $\tau_{CE}^L \leq \tau_{CE}$, in order to describe accurately the limit-state defined by $G(\boldsymbol{\theta}) = 0$.

5.2 | Online stage and error assessement

During the online stage, the optimized values λ^* of the λ parameters are used to generate the random variables such that a sufficient number of samples are in the failure domain. And the values of the limit-state function and its bounds are computed in the reduced bases computed along with the CE optimization which have been constructed to accurately represent the limit state function. The algorithm is given in Algorithm 5.

Then, the failure probability and the bounds are estimated by

$$\hat{P}_f^{rb,IS} = \frac{1}{N_{IS}} \sum_{n=1}^{N_{IS}} \mathbf{1}_{(G(\boldsymbol{\theta}^n)\leq 0)} \frac{f(\boldsymbol{\theta}^n)}{h_{opt}(\boldsymbol{\theta}^n)}, \quad \hat{P}_f^{+,IS} = \frac{1}{N_{IS}} \sum_{n=1}^{N_{IS}} \mathbf{1}_{(G_{rb}^-(\boldsymbol{\theta}^n)\leq 0)} \frac{f(\boldsymbol{\theta}^n)}{h_{opt}(\boldsymbol{\theta}^n)} \text{ and } \hat{P}_f^{-,IS} = \frac{1}{N_{IS}} \sum_{n=1}^{N_{IS}} \mathbf{1}_{(G_{rb}^+(\boldsymbol{\theta}^n)\leq 0)} \frac{f(\boldsymbol{\theta}^n)}{h_{opt}(\boldsymbol{\theta}^n)} \quad (60)$$

Algorithm 2 Pseudocode for the CE optimization algorithm

input: the PDF f, N_{CE} (number of samples used for the CE optimization), τ_{CE} (Acceptable error on the estimation of the limit state function : $G(\boldsymbol{\theta}) \leq G_k$), ρ a parameter in $[10^{-2}, 10^{-1}]$
output: $\mathcal{V}_{rb}^{0,n_{rb}}$, $\mathcal{S}_{rb}^{0,n_{rb}}$ and h_{opt}

Define $h_0 = f$. Set G_0 such that $G_0 > 0$.
Set $k = 0$ (iteration counter).
Generate a random sample $\boldsymbol{\theta}$ according to the probability density h_0. Compute $u_h(\boldsymbol{\theta})$ on the finite element mesh. Compute $\boldsymbol{\phi}^1 = u_h(\theta) - u_{dir}$ and $\boldsymbol{\zeta}^1 = \sigma_h(\boldsymbol{\theta}) - \sigma_{neu}(\boldsymbol{\theta})$. Initialize the reduced bases $\mathcal{V}_{rb}^{0,1} = \text{span}\,\{\boldsymbol{\phi}^1\}$ and $\mathcal{S}_{rb}^{0,1} = \text{span}\,\{\boldsymbol{\zeta}^1\}$. Set $n_{rb} = 1$.
while $G_k > 0$ **do**
  Set $k = k + 1$
  Generate N_{CE} random samples $\boldsymbol{\theta}^1, ..., \boldsymbol{\theta}^{N_{CE}}$ according to the probability density h_{k-1}
  for $n = 1, N_{CE}$ **do**
    Compute $G_{rb}(\boldsymbol{\theta}^n)$, $G_{rb}^-(\boldsymbol{\theta}^n)$, $G_{rb}^+(\boldsymbol{\theta}^n)$ and $\varepsilon_G(\boldsymbol{\theta}^n)$ by Algorithm (3)
    if $\varepsilon_G(\boldsymbol{\theta}^n) \geq \tau_{CE}$ and $G_{rb}^-(\boldsymbol{\theta}^n) \leq G_{k-1}$ **then**
      Compute $G(\boldsymbol{\theta}^n)$ on the finite element mesh. Increase the reduced bases $\mathcal{V}_{rb}^{0,n_{rb}}$ and $\mathcal{S}_{rb}^{0,n_{rb}}$. Set $n_{rb} = n_{rb} + 1$ and $G_{rb}(\boldsymbol{\theta}^n) = G(\boldsymbol{\theta}^n)$.
    end if
  end for
  Compute $G_k = \max(0, G_\rho)$, where G_ρ is the ρ-quantile of $G_{rb}(\boldsymbol{\theta}^1), ..., G_{rb}(\boldsymbol{\theta}^{N_{CE}})$
  Use $\boldsymbol{\theta}^1, ..., \boldsymbol{\theta}^{N_{CE}}$ to solve

$$\lambda^* = \underset{\lambda}{\text{argmax}} \frac{1}{N_{CE}} \sum_{n=1}^{N_{CE}} \mathbf{1}_{(G_{rb}(\boldsymbol{\theta}^n) \leq G_k)} \frac{f(\boldsymbol{\theta}^n)}{h_{k-1}(\boldsymbol{\theta}^n)} \ln h_\lambda(\boldsymbol{\theta}^n) \tag{58}$$

  Set $\lambda_k = \lambda^*$ and $h_k = h_{\lambda_k}$.
end while
Set $h_{opt} = h_k$

Algorithm 3 Pseudocode for the computation of $G_{rb}(\theta)$, $G_{rb}^-(\theta)$, $G_{rb}^+(\boldsymbol{\theta})$ and $\varepsilon_G(\boldsymbol{\theta}^n)$

input: $\boldsymbol{\theta}$, $\mathcal{V}_{rb}^{0,n_{rb}}$, $\mathcal{S}_{rb}^{0,n_{rb}}$
output: $G_{rb}(\theta)$, $G_{rb}^-(\theta)$, $G_{rb}^+(\boldsymbol{\theta})$ and $\varepsilon_G(\boldsymbol{\theta}^n)$

Compute $\mathbf{u}_{rb}(\boldsymbol{\theta})$ and $\mathbf{u}_{rb}^{aux}(\boldsymbol{\theta})$ in the reduced basis $\mathcal{V}_{rb}^{0,n_{rb}}$
Compute $\boldsymbol{\sigma}_{rb}^e(\boldsymbol{\theta})$ and $\boldsymbol{\sigma}_{rb}^{aux,e}(\boldsymbol{\theta})$ in the reduced basis $\mathcal{S}_{rb}^{0,n_{rb}}$
Compute $e_{rb}^-(\boldsymbol{\theta})$ and $e_{rb}^+(\boldsymbol{\theta})$ from (49)
Compute $\varepsilon_G(\boldsymbol{\theta}^n)$ from (57)
Compute $G_{rb}(\theta)$, $G_{rb}^-(\theta)$ and $G_{rb}^+(\boldsymbol{\theta})$ from (51) and (54)

6 | NUMERICAL EXAMPLES

6.1 | Example 1

In this first example, we aim at validating the algorithm by a comparison with a standard Monte-Carlo algorithm. We consider a plate with two rectangular holes proposed in[51]. The structure is submitted, in plane strain, to a normal traction $P = 10\,MPa$ applied along the vertical edge and the plate is considered to be composed of three different materials. The symmetry of the problem allows to study only one fourth of the plate as shown in Figure 2 .

The Poisson ratios are fixed $\nu_1 = \nu_2 = \nu_3 = 0.30$. The Young's moduli E_i are random independent variables such that their PDF is lognormal with a mean value $m_E = 200\,GPa$ and a standard deviation $\sigma_E = 40\,GPa$. The quantity of interest considered

Algorithm 4 Pseudocode for the last iteration of the CE optimization algorithm

input: the PDF f, N_{CE} (number of samples used for the CE optimization), τ_{CE}^{L} (Acceptable error on the estimation of the limit state function), $\mathcal{U}_{rb}^{0,n_{rb}}$, $S_{rb}^{0,n_{rb}}$ and h_{opt} the optimized density probability computed by Algorithm (2)
output: $\mathcal{U}_{rb}^{0,n_{rb}}$, $S_{rb}^{0,n_{rb}}$ and h_{opt}

Generate a random sample θ_1, ..., $\theta_{N_{CE}}$ according to the probability density h_{opt}
for $n = 1, ..., N_{CE}$ **do**
  Compute $G_{rb}(\boldsymbol{\theta}^n)$, $G_{rb}^{-}(\theta^n)$, $G_{rb}^{+}(\boldsymbol{\theta}^n)$ and $\varepsilon_G(\boldsymbol{\theta}^n)$ by Algorithm (3)
  if $G_{rb}^{+}(\boldsymbol{\theta}^n) > 0$ and $G_{rb}^{-}(\boldsymbol{\theta}^n) < 0$ **then**
    The RB accuracy is insufficient to certify the state of the structure
    if $\varepsilon_G(\boldsymbol{\theta}^n) > \tau_{CE}^{L}$ **then**
      Compute $G(\boldsymbol{\theta}^n)$ on the finite element mesh. Increase the reduced bases $\mathcal{U}_{rb}^{0,n_{rb}}$ and $\mathcal{S}_{rb}^{0,n_{rb}}$. Set $n_{rb} = n_{rb} + 1$ and $G_{rb}(\boldsymbol{\theta}^n) = G(\boldsymbol{\theta}^n)$.
    end if
  end if
end for
Use $\boldsymbol{\theta}^1$, ..., $\boldsymbol{\theta}^{N_{CE}}$ to solve

$$\lambda^* = \underset{\lambda}{\operatorname{argmax}} \frac{1}{N_{CE}} \sum_{n=1}^{N_{CE}} \mathbf{1}_{(G_{rb}(\boldsymbol{\theta}^n)\leq 0)} \frac{f(\boldsymbol{\theta}^n)}{h_{opt}(\boldsymbol{\theta}^n)} \ln h_{\lambda}(\boldsymbol{\theta}^n) \tag{59}$$

Set $h_{opt} = h_{\lambda^*}$

Algorithm 5 Pseudocode for IS MC Algorithm

input: the PDF f, N_{IS} (number of samples used for the IS), $\mathcal{U}_{rb}^{0,n_{rb}}$, $S_{rb}^{0,n_{rb}}$ and h_{opt} the optimized density probability computed by Algorithm (4)
output: $\hat{P}_f^{rb,IS}$, $\hat{P}_f^{+,IS}$, $\hat{P}_f^{-,IS}$

Set $N_f^{+} = 0$, $N_f = 0$, $N_f^{-} = 0$
for n= 1, N_{IS} **do**
  Generate $\boldsymbol{\theta}^n$ according to the probability density h_{opt}
  Compute $G_{rb}(\boldsymbol{\theta}^n)$, $G_{rb}^{-}(\theta^n)$ and $G_{rb}^{+}(\boldsymbol{\theta}^n)$ by Algorithm (3)
  if $G_{rb}^{+}(\boldsymbol{\theta}^n) \leq 0$ **then**
    Compute $w_n = \frac{f(\boldsymbol{\theta}^n)}{h_{opt}(\boldsymbol{\theta}^n)}$, $N_f^{+} = N_f^{+} + w_n$, $N_f^{rb} = N_f^{rb} + w_n$, $N_f^{-} = N_f^{-} + w_n$,
  else if $G_{rb}(\boldsymbol{\theta}^n) \leq 0$ **then**
    Compute $w_n = \frac{f(\boldsymbol{\theta}^n)}{h_{opt}(\boldsymbol{\theta}^n)}$, $N_f^{+} = N_f^{+} + w_n$, $N_f^{rb} = N_f^{rb} + w_n$,
  else if $G_{rb}^{-}(\boldsymbol{\theta}^n) \leq 0$ **then**
    Compute $w_n = \frac{f(\boldsymbol{\theta}^n)}{h_{opt}(\boldsymbol{\theta}^n)}$, $N_f^{+} = N_f^{+} + w_n$,
  end if
end for
Compute $\hat{P}_f^{rb,IS} = \frac{N_f}{N_{IS}}$, $\hat{P}_f^{+,IS} = \frac{N_f^{+}}{N_{IS}}$, $\hat{P}_f^{-,IS} = \frac{N_f^{-}}{N_{IS}}$

here is the average displacement on the line L_ω.

$$Q(\mathbf{u}(\boldsymbol{\theta}), \boldsymbol{\theta}) = \frac{1}{mes(L_\omega)} \int_{L_\omega} \mathbf{u}(\boldsymbol{\theta}).\mathbf{n}_\omega dl$$

The limit state function is given by

$$G(\boldsymbol{\theta}) = \bar{u} - Q(\mathbf{u}(\boldsymbol{\theta}), \boldsymbol{\theta})$$

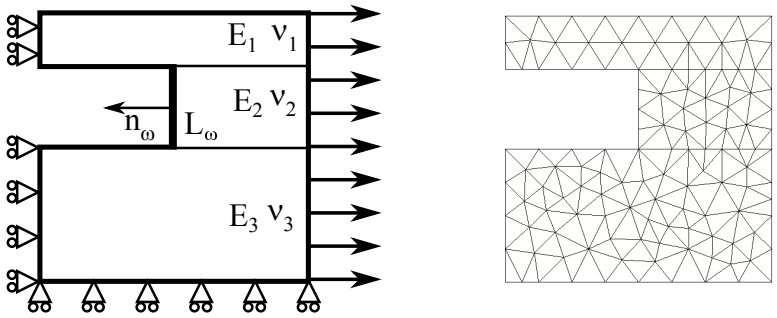

FIGURE 2 Example 1: Thick plate studied

where $\bar{u}$ is set to 7.3×10^{-5}. A standard Monte-Carlo method (SMC1) with $N^1_{MC} = 5 \times 10^4$ samples gives an estimate $\hat{P}_f = 2.68 \times 10^{-3}$ with a relative deviation $\delta = 8.6\%$. With $N^2_{MC} = 5 \times 10^5$ (SMC2) samples, we obtain $\hat{P}_f = 2.34 \times 10^{-3}$ with a relative deviation $\delta = 2.9\%$. For constructing the reduced bases and the CE optimization, we use the following parameters: $\rho = 0.1$, $N_{CE} = 500$, $\tau_{CE} = 7.3 \times 10^{-6}$ and $\tau^L_{CE} = 7.3 \times 10^{-7}$. At the end of the first step of optimization process (Algorithm 2), we obtain reduced bases of dimension 3, and the evolution of the PDF parameters presented in Table 3 . During the last step of optimization process (Algorithm 4) the dimension of the reduced bases increases to 5. The optimized PDF parameters are given in Table 4 .

k	G_k	$\tilde{m}_{E1}$	$\tilde{\sigma}_{E1}$	$\tilde{m}_{E2}$	$\tilde{\sigma}_{E2}$	$\tilde{m}_{E3}$	$\tilde{\sigma}_{E3}$
1	1.51×10^{-5}	200	40	200	40	200	40
2	3.16×10^{-6}	151.9	17.8	194.3	40.7	162.8	28.8
3	0	127.9	12.7	191.2	37.5	147.1	18.2

TABLE 3 Convergence of the CE optimization

k	G_k	$\tilde{m}_{E1}$	$\tilde{\sigma}_{E1}$	$\tilde{m}_{E2}$	$\tilde{\sigma}_{E2}$	$\tilde{m}_{E3}$	$\tilde{\sigma}_{E3}$
4	0	115.6	11.5	201.4	42.6	145.6	22.6

TABLE 4 Convergence of the CE optimization last iteration

Using the estimated optimal parameter vector $\lambda_4 = (115.6, 11.5, 201.4, 42.6, 145.6, 22.6)$ and the size 5 reduced bases with $N_{IS} = 5 \times 10^3$ samples gives an estimate of $\hat{P}_f^{rb,IS} = 2.48 \times 10^{-3}$, with a relative deviation $\delta = 5.1\%$. We obtain as well a lower bound of the failure probability $\hat{P}_f^{-,IS} = 2.30 \times 10^{-3}$ and an upper bound $\hat{P}_f^{+,IS} = 2.52 \times 10^{-3}$. We observe that, while 5×10^4 FOM resolutions are needed a standard MC method (SMC1) to obtain a relative deviation of $\delta = 8.6\%$, the proposed algorithm necessitates only 5 FOM resolutions to compute the RB and the IS optimized density during the offline stage and 5×10^3 ROM resolutions to compute the failure probability during the online stage. Compared to a standard MC method, the number of finite element simulations has been reduced by a factor 10^4 and the number of Monte-Carlo throws (during the online stage) has been reduced by a factor 10.

6.2 | Example 2

The second example concerns a composite structure composed of two layers linked by an interface as shown on Figure 3 . The structure is submitted, in plane strain, to a uniform normal traction P applied along the lower and upper surfaces. The deterministic parameters are the value of the traction $P = 9.2\ MPa$, the crack length $a = 0.15$, the length of the structure $L = 0.6$, the

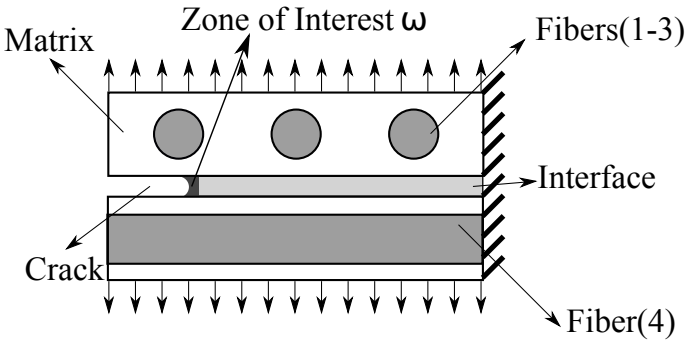

FIGURE 3 Example 2: Composite structure studied

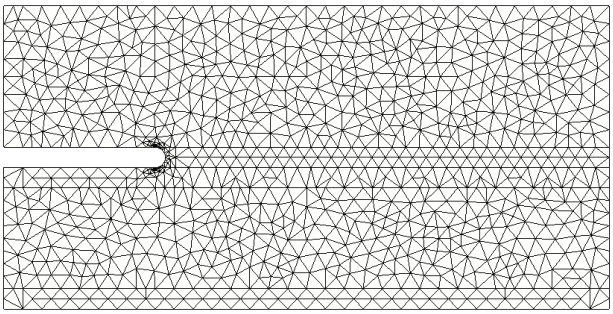

FIGURE 4 Example 2: Composite structure mesh

Random Variable	Distribution	Mean value (GPa)	Standard deviation (GPa)
E_{F1-3}	LogNormal	100	20
E_{F4}	LogNormal	20	4
E_M	LogNormal	10	2
E_I	LogNormal	1	0.2

TABLE 5 Example 2: Statistical properties of the random variables

thickness of the layers $e_L = 0.14$, the thickness of the interface $e_I = 0.02$, the radius of the fibers $r = 0.05$ and their positions. The random parameters, as defined in Table 5 , are the Young's moduli of the materials $\boldsymbol{\theta} = (E_{F1}, E_{F2}, E_{F3}, E_{F4}, E_M, E_I)$ (where F_i denotes the fibers, M the matrix and I the interface). The Poisson ratio's are set to 0.3. Figure 4 shows the 6-node triangular mesh used for the finite element analysis.

The Quantity of Interest is the mean value of the $\boldsymbol{\sigma}_{yy}$ over the subdomain ω and the limit state function is given by

$$G(\boldsymbol{\theta}) = R - \frac{1}{mes(\omega)} \int_{\omega} \boldsymbol{\sigma}_{yy}(\boldsymbol{\theta}) d\omega \tag{61}$$

where R is a deterministic value set to $180\ MPa$.

A standard Monte-Carlo method (SMC1) with 10^7 samples gives an estimate $\hat{P}_f = 3.16 \times 10^{-4}$ with a relative deviation $\delta = 1.8\%$. For constructing the reduced bases and the CE optimization we use the following parameters: $\rho = 0.1$, $N_{CE} = 500$, $\tau_{CE} = 18\ MPa$ and $\tau_{CE}^L = 1.8\ MPa$. The optimization process converges in 4 iterations (Algorithms 2 and 4) and we obtain

reduced bases of dimension 9. The optimized PDF parameters are given in Table 6 . Using optimized PDF parameters and the size 9 reduced bases with $N_{IS} = 10^4$ samples gives an estimate of $\hat{P}_f^{rb,IS} = 3.19 \times 10^{-4}$, with a relative deviation $\delta = 2.9\%$. We obtain as well a lower bound of the failure probability $\hat{P}_f^{-,IS} = 2.81 \times 10^{-4}$ and an upper bound $\hat{P}_f^{+,IS} = 3.72 \times 10^{-4}$. To compare with a Monte-Carlo simulation performed by a RB without CE optimization, we run the Monte-Carlo simulation with the reduced basis approximation computed during the offline step and the initial PDF f, and we compute the failure probability $\hat{P}_f$ with the Monte-Carlo estimator (Equation 15). The number of samples used is $N_{MC} = 4 \times 10^6$, and we obtain $\hat{P}_f = 3.12 \times 10^{-4}$, with a relative deviation $\delta = 2.8\%$. In this case, we have reduced the number of computations of the ROM during the online phase by a factor 4×10^2.

Random Variable	E_{F1}	E_{F2}	E_{F3}	E_{F4}	E_M	E_I
Mean Value (GPa)	95.9	97.8	113.0	15.76	8.10	1.84
Standard deviation (GPa)	19.6	19.4	27.2	2.88	2.19	0.25

TABLE 6 Example 2: optimized PDF parameters

Two series of tests are performed to check the robustness of the failure probability estimate. The algorithm is run 10 times with the following parameters $\rho = 0.1$, $N_{CE} = 500$, $N_{IS} = 10^4$, $\tau_{CE} = 18\,MPa$, $\tau_{CE}^L = 1.8\,MPa$, then with the same parameters but with a smaller tolerance $\tau_{CE} = 1.8\,MPa$, $\tau_{CE}^L = 0.18\,MPa$. The evolution of the ratio $r = \frac{\hat{P}_f^{rb,IS}}{\hat{P}_f}$ for the two set of computations is shown in Figure 5 . It can be observed that the ratio is very sharp varying from 0.9 to 1.1 and that the estimate becomes more reliable when the tolerance decreases. For $\tau_{CE}^L = 1.8\,MPa$ the size of the reduced bases varies from 9 to 10 for the different runs and for $\tau_{CE}^L = 1.8\,MPa$ the size of the reduced bases varies from 15 to 17. Figure 6 displays the variation the failure's probability bounds ($\hat{P}_f^{+,IS}$ and $\hat{P}_f^{-,IS}$) for 10 runs and shows that the bounds gaps become narrower as the tolerance decreases.

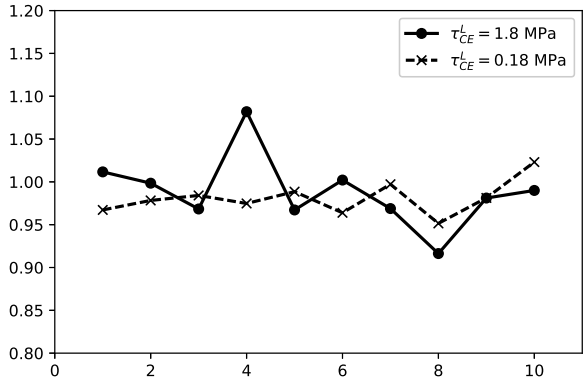

FIGURE 5 Evolution of $r = \frac{\hat{P}_f^{rb,IS}}{\hat{P}_f}$ for 10 runs

Figure 7 shows the relative deviation δ as a function of N_{IS} the number of sampling points. In this case, we have built the optimized PDF and the reduced basis with the following parameters: $\rho = 0.1$, $N_{CE} = 500$, $\tau_{CE} = 0.18\,MPa$, $\tau_{CE}^L = 0.018\,MPa$, leading to $n_{rb} = 28$. It can be observed that in this case 10^3 samples are sufficient to obtain a relative deviation inferior to 10%.

Table 7 shows the evolution of the failure probability and the evolution of the number of the elements in the reduced bases when loading P decreases. The algorithm is run with the following parameters: $\rho = 0.1$, $N_{CE} = 500$, $N_{IS} = 10^4$, $\tau_{CE} = 1.8\,MPa$, $\tau_{CE}^L = 0.18\,MPa$. The failure probability decreases rapidly with the force drop. However, it can be seen that there is

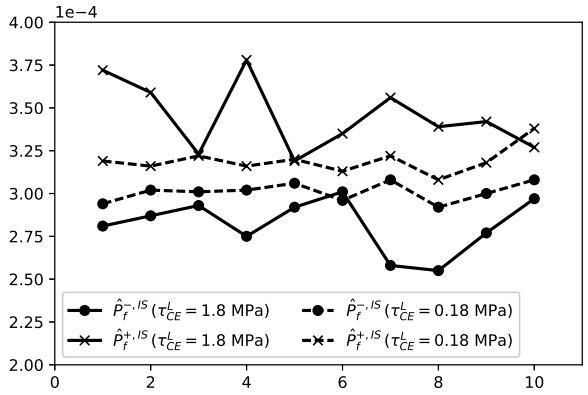

FIGURE 6 Variation of the failure's probability bounds ($\hat{P}_f^{+,IS}$ and $\hat{P}_f^{-,IS}$) for 10 runs

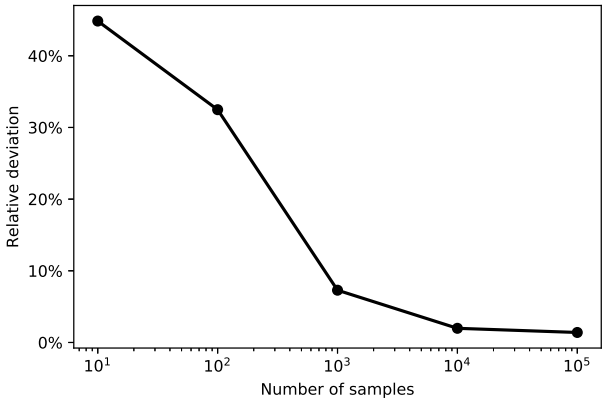

FIGURE 7 Evolution of the relative deviation δ as a function of N_{IS}

no increase of the number of elements in the reduced bases and that less than 20 FE computations are sufficient to accurately estimate the failure probability. The relative deviation remains stable between 3% and 5%. If we consider that 10^9 finite element computations would be necessary to estimate the 7.4×10^{-8} failure probability we observe that the number of finite element computations is reduced by a factor 5×10^7 and the number of computations in the reduced basis by a factor 10^5.

P (MPa)	9.2	9.0	8.8	8.6	8.4	8.2
$\hat{P}_f^{rb,IS}$	3.2×10^{-4}	8.4×10^{-5}	1.89×10^{-5}	3.4×10^{-6}	5.6×10^{-7}	7.4×10^{-8}
$\hat{P}_f^{+,IS}$	3.7×10^{-4}	8.6×10^{-5}	1.94×10^{-5}	3.6×10^{-6}	6.3×10^{-7}	7.8×10^{-8}
$\hat{P}_f^{-,IS}$	2.8×10^{-4}	8.1×10^{-5}	1.86×10^{-5}	3.3×10^{-6}	5.1×10^{-7}	7.1×10^{-8}
Relative deviation δ (%)	2.9	2.9	4.0	3.6	4.7	3.0
CE number of iterations	4	4	5	5	5	6
N_s^{max}	15	16	17	18	16	19

TABLE 7 Computed failure probability and bounds

7 | CONCLUSIONS

In this paper, we have developed an adaptive computational strategy aiming to compute the failure probability of a structure in the context of rare events simulations. We use a cross-entropy method to construct an optimized probability density function for the importance sampling estimator. A surrogate model based on a reduced basis approach is constructed during the cross-entropy optimization and the reduced basis vectors are chosen in order to control the quality of the estimation of the limit state function.

In the numerical examples, we show that the algorithm permits estimating failure probabilities from 10^{-4} to 10^{-7} with less than 20 finite elements computations during the offline phase and only 10^4 calls to the surrogate model during the online phase. Finally, bounds of the Monte-Carlo estimator are computed which permit to assess the quality of the reduced basis. It is interesting to note that a possible improvement of the algorithm would be to use the bounds of the Monte-Carlo estimator to add vectors in the reduced basis during the online process in order to prescribe certified bounds for the estimate of the failure probability.

References

1. O. Ditlevsen and H.O. Madsen. Structural reliability methods. Wiley, New York, 1996.
2. M Lemaire, A Chateauneuf, and JC Mitteau. Structural reliability. ISTE, 2010.
3. A.M. Hasofer and N.C. Lind. An exact and invariant first order reliability format. J. Eng. Mech. - ASCE, 1(100):111–121, 1974.
4. R. Rackwitz and B. Fiessler. Structural reliability under random load sequences. Computer and Structures, 5(9):484–494, 1979.
5. A. Der Kiureghian and M. de Stefano. Efficient algorithm for second-order reliability analysis. J. Eng. Mech., 12(117):37–49, 1991.
6. T. Haukaas and A. Der Kiureghian. Strategies for finding the design point in non-linear finite element reliability analysis. Probabilistic Engineering Mechanics, (21):133–147, 2006.
7. L Gallimard. Error bounds for the reliability index in finite element reliability analysis. International Journal for Numerical Methods in Engineering, 87(8):781–794, 2011.
8. L Gallimard, P Vidal, and O Polit. Coupling finite element and reliability analysis through proper generalized decomposition model reduction. International Journal for Numerical Methods in Engineering, 95(13):1079–1093, 2013.
9. P Colombi and L Faravelli. Stochastic finite elements via response surface: fatigue crack growth problems. In C. Guedes Soares, editor, Probabilistic Methods for Structural Design, pages 313–338. Springer, Netherlands, Dordrecht, 1997.
10. M Pendola, A Mohamed, M Lemaire, and P Hornet. Combination of finite element and reliability methods in nonlinear fracture mechanics. Reliability Engineering and System Safety, 70(1):15–27, 2000.
11. B Sudret and A. Der Kiureghian. Comparison of finite element reliability methods. Prob. Eng. Mech., 17:337–348, 2002.
12. M. Berveiller, B. Sudret, and M. Lemaire. Stochastic finite elements: a non intrusive approach by regression. Eur. J. Comput. Mech., 15(1-3):81–92, 2006.
13. G. Blatman and B. Sudret. An adaptive algorithm to build up sparse polynomial chaos expansions for stochastic finite element analysis. Prob. Eng. Mech., 25(2):183–197, 2010.
14. P.S. Mohan, P.B. Nair, and A.J. Keane. Multi-element stochastic reduced basis methods. Comput. Methods Appl. Mech. Eng., 197:1495–1506, 2008.
15. S. Boyaval, C. Le Bris, Y. Maday, N. C. Nguyen, and A. T. Patera. Reduced basis approach for variational problems with stochastic parameters: application to heat conduction with variable robin coefficient. Comp. Meth. in Applied Mech. and Engrg., 198(41-44):3187–3206, 2009.

16. S. Boyaval, C. Le Bris, T. Lelièvre, Y. Maday, N. C. Nguyen, and A. T. Patera. Reduced basis techniques for stochastic problems. Arch. Comput. Methods Engrg., 17:435–454, 2010.

17. M. Grigoriu. Reduced order models for random functions application to stochastic problems. Appl. Math. Model., 33:161–175, 2009.

18. E. Florentin and P. Dìez. Adaptive reduced basis strategy based on goal oriented error assessment for stochastic problems. Comp. Meth. in Applied Mech. and Engrg., 225-228:116–127, 2012.

19. B. Haasdonk, K. Urban, and B. Wieland. Reduced basis methods for parametrized partial differential equations with stochastic influences using the Karhunen Loeve expansion. SIAM/ASA J. Unc. Quant., 1:79–105, 2013.

20. P Chen and A Quarteroni. Accurate and efficient evaluation of failure probability for partial different equations with random input data. Comput. Methods Appl. Mech. Eng., 267:233–260, 2013.

21. L Gallimard, E Florentin, and D Ryckelynck. Towards error bounds of the failure probability of elastic structures using reduced basis models. International Journal for Numerical Methods in Engineering, 112(9):1216–1234, 2017.

22. J Morio, M Balesdent, D Jacquemart, and C Vergé. a survey of rare event simulation methods for static input-output models. Simulation Modelling Partice and Theory, 49:287–304, 2014.

23. Tito Homem-de-Mello. A study on the cross-entropy method for rare-event probability estimation. INFORMS Journal on Computing, 19(3):381–394, 2007.

24. J Li, J Li, and D Xiu. An efficient surrogate-based method for computing rare failure probability. Journal of Computational Physics, 230(24):8683 – 8697, 2011.

25. Mathieu Balesdent, Jerome Morio, and Julien Marzat. Kriging-based adaptive importance sampling algorithms for rare event estimation. Structural Safety, 44:1–10, 2013.

26. B Peherstorfer, B Kramer, and C Willcox. Multifidelity preconditioning of the cross-entropy method for rare event simulation and failure probability estimation. SIAM/ASA Journal on Uncertainty Quantification, 6(2):737–761, 2018.

27. P. Kerfriden, J. J. Rodenas, and S. P. A. Bordas. Certification of projection-based reduced order modelling in computational homogenisation by the constitutive relation error. Int. J. Numer. Meth. in Engng., 97(6):395–422, 2014.

28. N. C. Nguyen, K Vero, and A. T. Patera. Certified real-time solution of parametrized partial differential equations. In S. Yip, editor, Handbook of Materials Modeling, pages 1523–1558. Springer, Netherlands, 2005.

29. R.G. Ghanem and P.D. Spanos. Stochastic Finite Elements: A spectral Approach, Revised Edition. Dover, New York, 2003.

30. L Chamoin, E Florentin, S Pavot, and V Visseq. Robust goal-oriented error estimation based on the constitutive relation error for stochastic problems. Computers and Structures, 106-107:189 – 195, 2012.

31. A Mohamed, M Lemaire, JC Mitteau, and E Meister. Finite element and reliability: a method for compound variables: application on a cracked heating system. Nuclear engineering and design, 185(2-3):185–202, 1998.

32. R.E. Melchers. Importance sampling in structural systems. Structural Safety, (6):3–10, 1989.

33. S. Engelund and R. Rackwitz. A benchmark study on importance sampling techniques in strucural reliability. Struct. Safe., 12(4):255–276, 1993.

34. G.C. Orsak and B. Aazhang. A class of optimum importance sampling strategies. Inf. Sci., 84(1-2):139–160, 1995.

35. R. Y. Rubinstein. The cross-entropy method for combinatorial and continuous optimization. Methodology Comput. Appl. Probab., 2:127–190, 1999.

36. Pieter-Tjerk De Boer, Dirk P. Kroese, Shie Mannor, and Reuven Y. Rubinstein. A tutorial on the cross-entropy method. Annals of Operation Research, 134:19–67, 2005.

37. D. B. P. Huynh and A. T. Patera. Reduced basis approximation and a posteriori error estimation for stress intensity factors. International Journal for Numerical Methods in Engineering, 72(10):1219–1259, 2007.

38. G. Rozza, D. B. P. Huynh, and A. T. Patera. Reduced basis approximation and a posteriori error estimation for affinely parametrized elliptic coercive partial differential equations. Arch Comput Methods Eng, 15:229–275, 2008.

39. I. Martini, G. Rozza, and B. Haasdonk. Reduced basis approximation and a-posteriori error estimation for the coupled stokes-darcy system. Advances in Computational Mathematics, 41(5):1131Ăćâ Ćňâ ĂIJ1157, 2015.

40. JD Yang, DW Kelly, and JD Isles. A posteriori pointwise upper bound error estimates in the finite element method. International journal for numerical methods in engineering, 36(8):1279–1298, 1993.

41. S. Prudhomme and J.T. Oden. On goal-oriented error estimation for elliptic problems : application to the control of pointwise errors. Comp. Meth. in Applied Mech. and Engrg., 176:313–331, 1999.

42. S. Ohnimus, E. Stein, and E. Walhorn. Local error estimates of fem for displacements and stresses in linear elasticity by solving local neumann problems. Int. J. Numer. Meth. in Engng., 52:727–746, 2001.

43. S. Prudhomme, J.T. Oden, T. Westermann, J. Bass, and M. E. Botkin. Practical methods for a posteriori error estimation in engineering applications. Int. J. Numer. Meth. in Engng., 56:1193–1224, 2003.

44. P. Ladevèze, F. Pled, and L. Chamoin. New bounding techniques for goal-oriented error estimation applied to linear problems. International Journal for Numerical Methods in Engineering, 93(13):1345–1380, 2012.

45. L Machiels, Y. Maday, and A.T. Patera. Output bounds for reduced-order approximations of elliptic partial differential equations. Comp. Meth. in Applied Mech. and Engrg., 190:3413–3426, 2001.

46. D Ryckelynck, L Gallimard, and S Jules. Estimation of the validity domain of hyper-reduction approximations in generalized standard elastoviscoplasticity. Advanced Modeling and Simulation in Engineering Sciences, 2(1):1–19, 2015.

47. KC Hoang, P Kerfriden, and SPA Bordas. A fast, certified and tuning free two-field reduced basis method for the metamodelling of affinely-parametrised elasticity problems. Computer Methods in Applied Mechanics and Engineering, 298:121–158, 2016.

48. L Gallimard and D Ryckelynck. A posteriori global error estimator based on the error in the constitutive relation for reduced basis approximation of parametrized linear elastic problems. Applied Mathematical Modelling, 40:4271–4284, 2016.

49. L. Gallimard. A constitutive relation error estimator based on traction-free recovery of the equilibrated stress. Int. J. for Num. Meth. in Engrg., 78(4):460–482, 2009.

50. L Gallimard. Evaluation of the local quality of the von mises's stress and l2-norm of the stress. Engineering Computations, 68(7/8):876–897, 2006.

51. J. Peraire and A. Patera. Bounds for linear-functional outputs of coercive partial differential equations: local indicators and adaptive refinement. In P. Ladevèze and J.T. Oden, editors, Advances in Adaptive Computational Methods, volume 47 of Studies in Applied Mechanics, pages 199–216. Elsevier, 1998.